

A three-parameter dispersion relationship for Biot's fast compressional wave in a marine sediment

Michael J. Buckingham^{a)}

Marine Physical Laboratory, Scripps Institution of Oceanography, University of California, San Diego, 9500 Gilman Drive, La Jolla, California 92093-0238

(Received 18 November 2002; accepted for publication 15 December 2003)

When the bulk and shear moduli of the mineral frame are set to zero, the full Biot theory of wave propagation in a porous medium such as a marine sediment reduces to Williams' "effective density fluid" (EDF) model [J. Acoust. Soc. Am. **110**, 2276–2281 (2001)]. Although eight material variables appear in the EDF model, it is in fact tightly constrained, possessing just three degrees of freedom: the phase speeds in the limits of low and high frequency, c_0 and c_∞ , respectively, and a transition frequency, f_T , separating the low- and high-frequency regimes. In this paper, an algebraic approximation to the EDF model is formulated, which is termed the "modified viscous fluid" (MVF) model, involving only the three parameters (c_0, c_∞, f_T) . Expressions are developed for (c_0, c_∞, f_T) in terms of the eight material properties; and a comparison of the MVF and EDF dispersion curves is performed, showing that they are essentially identical at all frequencies. Apart from its computational simplicity, the MVF model provides insight into the effect of each material parameter on the shape of the dispersion curves. For instance, the transition frequency scales as the ratio of the pore–fluid viscosity to the permeability, but neither the viscosity nor the permeability affects the limiting phase speeds c_0 and c_∞ . © 2004 Acoustical Society of America.

[DOI: 10.1121/1.1646672]

PACS numbers: 43.30.Ma, 43.20.Jr. [WMS]

Pages: 769–776

I. INTRODUCTION

In a recent article, Williams¹ developed an "effective density fluid" (EDF) model of acoustic wave propagation in an unconsolidated, saturated porous medium such as a marine sediment. Based on the classical theory of Biot^{2,3} for wave propagation in a two-phase, porous medium, the EDF model is a reduced version of Biot's original formulation in which the (complex) frame bulk modulus and the (complex) frame shear modulus have been set to zero. Neglect of the elastic frame (in the context of Biot's theory) amounts to treating the porous medium as a homogeneous fluid, capable of supporting Biot's "fast" compressional wave but not the "slow" wave nor the shear wave of the full Biot theory.

Experimentally, the shear wave is observed to be weak⁴ and the slow wave is negligible, if present at all,^{5–10} in saturated, unconsolidated granular materials. For such materials, the "effective fluid" representation is probably reasonable. Indeed, in an alternative to the Biot theory, developed recently by Buckingham,¹¹ in which the internal stresses arise from intergranular traction rather than pore–fluid viscosity, the absence of a mineral frame has been taken as a defining feature of an unconsolidated sediment. Two types of wave emerge from Buckingham's model, a fast compressional wave and a shear wave (even though there is no elastic frame), the latter arising naturally from the rigidity introduced into the medium by the intergranular interactions.

Although the number of parameters involved in the EDF model is four less than in the full Biot theory, the final result

for the complex sound speed [Eqs. (13) and (14), in Williams¹] still involves eight variables, as listed in Table I, which describe material properties. At first sight, so many variables would seem to suggest that the EDF dispersion curves are highly adjustable, but this is not the case. As may be seen in Figs. 2 and 3 of Williams¹ showing the frequency dependence of the phase speed and attenuation, the EDF dispersion curves exhibit just three characteristic features: (1) a low-frequency limit to the phase speed, c_0 ; (2) a high-frequency limit to the phase speed, c_∞ ; and (3) a transition frequency, f_T , separating the low- and high-frequency regimes in the phase speed and attenuation curves. As frequency increases through f_T , the attenuation switches from a low-frequency power-law scaling of f^2 to a high-frequency scaling of $f^{1/2}$ and the phase speed begins to increase above the low-frequency value, c_0 , to approach asymptotically the limiting high-frequency value, c_∞ . If the complex sound speed can be represented by just the three parameters (c_0, c_∞, f_T) , it follows that the eight material variables shown in Table I do not affect the predictions of the EDF model independently, but instead these eight variables must collapse into the three parameters (c_0, c_∞, f_T) .

The phase speed and attenuation curves in Figs. 2 and 3 of Williams¹ are reminiscent of the complex sound speed in a purely viscous fluid¹² or, equivalently, a Voigt solid.¹³ The only difference is that, in a viscous fluid, the phase speed diverges at high frequencies as $f^{1/2}$, which is tantamount to saying that c_∞ is infinite, as opposed to the EDF model where c_∞ is finite. Otherwise, the EDF model yields dispersion curves exhibiting the familiar characteristics of viscous dissipation. This is perhaps not surprising, since the only loss mechanism in the EDF model, and indeed in the full Biot

^{a)}Also affiliated with the Institute of Sound and Vibration Research, The University, Southampton SO 17 1BJ, United Kingdom. Electronic mail: mjb@mpl.ucsd.edu

TABLE I. Nomenclature and values [after Williams (Ref. 1)] for the eight material properties relevant to the EDF model.

Material property	Symbol	Value
Porosity	β	0.4
Density of mineral grains	ρ_s	2650 kg/m ³
Bulk modulus of mineral grains	K_r	3.6×10 ¹⁰ Pa
Density of pore fluid	ρ_f	1000 kg/m ³
Bulk modulus of pore fluid	K_f	2.25×10 ⁹ Pa
Viscosity of pore fluid	η	0.001 kg/m s
Permeability	κ	1.0×10 ⁻¹⁰ m ²
Tortuosity	α	1.25

theory, is viscosity of the pore fluid. As discussed below, after introducing a minor modification, the expression for the complex sound speed in a viscous fluid is found to match accurately the phase speed and attenuation from the EDF model at all frequencies.

In this article, the predictions of the EDF model are summarized and compared with those of the modified viscous fluid (MVF) model,¹⁴ the latter involving only the three parameters (c_0, c_∞, f_T). Explicit expressions are derived for these three parameters in terms of the eight material variables listed in Table I. It turns out that the MVF model is, for practical purposes, indistinguishable from the EDF model and, being purely algebraic, is easier to compute. The principal advantage of the MVF model, however, is that it provides an elementary means of identifying the effects of the material variables on the main features of the EDF dispersion curves. For example, the limiting low- and high-frequency phase speeds, c_0 and c_∞ , respectively, are independent of both the permeability, κ , and the pore–fluid viscosity, η ; these two material variables affect the dispersion curves *only* as the ratio (η/κ), which appears *only* as a linear scaling factor in the expression for the transition frequency, f_T . Obviously, it follows that if the permeability and viscosity are scaled by the same factor, the dispersion curves from the EDF model remain invariant.

Before proceeding with the development of the MVF model, it is as well to point out that many authors have applied the full Biot theory to the interpretation of wave propagation data obtained from a wide variety of porous media, including consolidated and unconsolidated marine sediments (for a bibliography covering much of the relevant material that had been published up until 1989, see the monograph by Stoll¹⁵). In other applications, the Biot model has been incorporated into a parabolic equation for the purpose of estimating acoustic propagation loss in ocean channels overlying poroelastic layers;¹⁶ and, in a rather different arena, the Biot theory has been applied in the interpretation of medical-acoustics data, particularly on ultrasonic wave propagation in water-saturated cancellous and cortical bone.¹⁷ Several authors have investigated the sensitivity of the Biot dispersion curves to variations in the material parameters of sediments, a recent example being the paper by Mu *et al.*,¹⁸ which includes references to earlier work on a similar theme. Apart from the paper by Williams,¹ however, little has been done in the way of reducing the Biot theory to a form that provides simple physical insights into the predicted dispersion relationships for unconsolidated marine

sediments. This is the aim of the following discussion.

II. SUMMARY OF THE EDF MODEL

In the following account of the EDF model, the nomenclature adopted is similar to that used by Williams.¹ As the symbols representing the eight material variables are identified in Table I, not all of their definitions are repeated in the text.

According to Eq. (13) in Williams,¹ the complex sound speed, c , in the two-phase, EDF medium is given by

$$\frac{1}{c} = \sqrt{\frac{\rho_{\text{eff}}}{H}}, \quad (1)$$

where

$$H = \left[\frac{(1-\beta)}{K_r} + \frac{\beta}{K_f} \right]^{-1} \quad (2)$$

is the bulk modulus (i.e., the reciprocal of the compressibility) of the composite material. From an inspection of Williams' Eq. (14), it is clear that the complex effective density, ρ_{eff} , can be expressed in the form

$$\rho_{\text{eff}}(\omega\tau_0) = \rho_f \left\{ \frac{\rho_1 + i\beta\rho \frac{F(\omega\tau_0)}{\omega\tau_0}}{\rho_2 + i\beta\rho_f \frac{F(\omega\tau_0)}{\omega\tau_0}} \right\}, \quad (3)$$

where ω is angular frequency and ρ is the bulk density of the two-phase medium, as given by the following linear combination of the densities of the mineral grains and pore fluid:

$$\rho = \beta\rho_f + (1-\beta)\rho_s. \quad (4)$$

The two parameters $\rho_{1,2}$ in Eq. (3) have units of density and are given by the expressions

$$\rho_1 = \alpha(1-\beta)\rho_s + \beta(\alpha-1)\rho_f, \quad (5a)$$

$$\rho_2 = \beta(1-\beta)\rho_s + (\alpha-2\beta+\beta^2)\rho_f. \quad (5b)$$

Clearly, the tortuosity, α , affects ρ_1 and ρ_2 but appears nowhere else in the EDF model. Note that, in Eq. (3), the frequency dependence of ρ_{eff} is contained exclusively in the term $(\omega\tau_0)^{-1}F(\omega\tau_0)$, where $\omega\tau_0$ is a dimensionless frequency, and the normalizing time is

$$\tau_0 = \frac{\kappa\rho_f}{\eta}. \quad (6)$$

It is to be emphasized that the permeability, κ , and pore–fluid viscosity, η , appear in the EDF model only through τ_0 , and hence, as mentioned earlier, they affect the dispersion curves only as the ratio κ/η . Moreover, τ_0 appears only as the normalizing factor in the dimensionless frequency ($\omega\tau_0$). A similar but not identical normalization was used by Biot^{2,3} in the form of a “characteristic frequency” $f_c = \beta/(2\pi\tau_0)$, which he used when plotting compressional wave speeds as a function of frequency.

The function F in Eq. (3) was introduced by Biot³ to account for the departure from Poiseuille flow through the pores of the mineral frame as frequency increases. He derived the expression

$$F(\varepsilon) = \frac{(\varepsilon/4)T(\varepsilon)}{1 - (2i/\varepsilon)T(\varepsilon)}, \quad (7)$$

in which

$$T(\varepsilon) = \frac{-\sqrt{i}J_1(\varepsilon\sqrt{i})}{J_0(\varepsilon\sqrt{i})}, \quad (8a)$$

where J_n are Bessel functions of the first kind of order $n = 0, 1$. The argument of F is

$$\varepsilon = a \sqrt{\frac{\omega \rho_f}{\eta}}, \quad (8b)$$

where a is the pore size parameter, an expression for which has been derived by Johnson, Koplik, and Dashen:¹⁹

$$a = \sqrt{\frac{8\alpha\kappa}{\beta}}. \quad (9)$$

On combining Eqs. (8b) and (9), it is evident that

$$\varepsilon = \varepsilon(\omega\tau_0) = \sqrt{\frac{8\alpha}{\beta}} \omega\tau_0, \quad (10)$$

thus confirming that frequency always appears in the EDF dispersion relationship as the dimensionless product $\omega\tau_0$.

Equations (1)–(10) constitute the complete “fluid” Biot, or EDF, model, although Eq. (3) for the effective density is formulated slightly differently from the version in Williams¹ in order to make explicit the dependence on the normalized frequency $\omega\tau_0$. Later, it will become clear that the transition frequency, f_T , is proportional to $(\tau_0)^{-1}$, from which it follows that the only role of the permeability and the pore–fluid viscosity is to scale f_T by the factor η/κ . This scaling amounts to a simple translation of the EDF dispersion curves along the (logarithmic) frequency axis, leaving their shapes unchanged.

To express f_T in terms of the material properties, it will be necessary to compare the MVF and EDF models, a procedure that will require the Taylor expansion of Eq. (1) to first order in the normalized frequency, $\omega\tau_0$. The series is straightforward to derive, although care must be taken to expand the function T in Eq. (8) to fourth order in ε , which then yields the function F to second order in ε :

$$F(\varepsilon) = 1 + \frac{i\varepsilon^2}{4} - \dots. \quad (11)$$

When Eq. (11) is combined with Eq. (1), and after a little more algebra, the following expansion, to first order in $\omega\tau_0$, for the reciprocal of the complex sound speed is obtained:

$$\frac{1}{c} = \sqrt{\frac{\rho}{H}} \left\{ 1 + \frac{i\omega\tau_0}{2\beta} \left(\frac{\rho_2}{\rho_f} - \frac{\rho_1}{\rho} \right) + \dots \right\}. \quad (12)$$

This expression, and hence also Eq. (3), can be seen to correspond to a time dependence of the form $\exp(-i\omega t)$. It is obvious from Eq. (12) that, in the limit of low frequency, the complex sound speed becomes real and is given by

$$c_0 = \sqrt{\frac{H}{\rho}}, \quad (13)$$

which is identical to Wood’s equation²⁰ for a suspension of noninteracting particles in a fluid. In his original papers, Biot^{2,3} used c_0 as a normalizing factor in plots of the phase speed of the dilatational waves of the first and second kind (i.e., the fast and slow compressional waves).

III. THE MVF MODEL

Wave propagation in a viscous fluid or a Voigt solid is governed by a linear, second-order, partial differential equation of the form^{12,13}

$$\nabla^2 \psi - \frac{1}{c_0^2} \dot{\psi} + \tau \nabla^2 \dot{\psi} = 0, \quad (14)$$

where ∇^2 is the Laplacian, ψ is the velocity potential, the coefficient τ is a viscous dissipation time, and c_0 is still the phase speed in the medium in the limit of low frequency. From the solution of this equation, the reciprocal of the complex sound speed, \bar{c} , in a viscous fluid may be expressed as

$$\frac{1}{\bar{c}} = \frac{1}{c_0} \frac{\sqrt{1 + i\omega\tau}}{[1 + \omega^2\tau^2]^{1/2}}, \quad (15)$$

where, for consistency with the EDF model, the time-dependence has been chosen as $\exp(-i\omega t)$, as may be deduced from the plus (+) sign preceding the imaginary term under the radical in the numerator. Equation (15) is a well-known expression, which shows a frequency dependence that exhibits two regimes, high and low, separated by a transition frequency $f_T = (2\pi\tau)^{-1}$.

By taking its real and imaginary parts, Eq. (15) yields the following expressions for phase speed, \bar{c}_p , and attenuation, $\bar{\alpha}_p$, in a viscous fluid:

$$\bar{c}_p = [\Re(\bar{c}^{-1})]^{-1} = \frac{\sqrt{2}c_0\sqrt{1 + \omega^2\tau^2}}{[1 + \sqrt{1 + \omega^2\tau^2}]^{1/2}} \rightarrow \begin{cases} c_0, & \text{for } \omega\tau \ll 1, \\ c_0\sqrt{2\omega\tau}, & \text{for } \omega\tau \gg 1, \end{cases} \quad (16)$$

and

$$\bar{\alpha}_p = [\omega\Im(\bar{c}^{-1})] = \frac{\omega}{\sqrt{2}c_0} \frac{[\sqrt{1 + \omega^2\tau^2} - 1]^{1/2}}{\sqrt{1 + \omega^2\tau^2}} \rightarrow \begin{cases} \frac{\omega^2\tau}{2c_0}, & \text{for } \omega\tau \ll 1, \\ \frac{1}{c_0} \sqrt{\frac{\omega}{2\tau}}, & \text{for } \omega\tau \gg 1. \end{cases} \quad (17)$$

Clearly, the high- and low-frequency limiting forms of the attenuation in Eq. (17) are identical to those of the EDF model, as exemplified in Fig. 3 of Williams.¹ The low-frequency limit of the phase speed in Eq. (16) also conforms with the EDF model, but at high frequencies \bar{c}_p in Eq. (16) scales as $\omega^{1/2}$, unlike the phase speed from the EDF model, which, as illustrated in Williams’ Fig. 2, asymptotes to a finite limiting value, c_∞ .

The full frequency dependence of the EDF model, including the high-frequency limiting behavior of the phase speed, may be reproduced by making Eq. (15) a little more general:¹⁴

$$\frac{1}{\bar{c}} = \left(\frac{1}{c_0} - \frac{1}{c_\infty} \right) \frac{\sqrt{1 + i\omega\tau}}{[1 + \omega^2\tau^2]^{1/2}} + \frac{1}{c_\infty}, \quad (18)$$

which is the form referred to earlier as the modified viscous fluid (MVF) model. [N.B.: As in Eq. (15), the plus (+) sign preceding the imaginary term under the radical in Eq. (18) corresponds to an implied time dependence of the form $\exp(-i\omega t)$, consistent with the convention used in the EDF model. This accounts for the difference between Eq. (18) and its counterpart, Eq. (25), in Ref. 14, where the imaginary term is preceded by a minus (-) sign, corresponding to a time dependence of the form $\exp(+i\omega t)$.] By an extension of Eqs. (16) and (17), the phase speed and attenuation from the MVF model may be expressed as follows:

$$\bar{c}_p = \left[\frac{1}{\sqrt{2}} \left(\frac{1}{c_0} - \frac{1}{c_\infty} \right) \left\{ \frac{\sqrt{1 + \omega^2\tau^2} + 1}{1 + \omega^2\tau^2} \right\}^{1/2} + \frac{1}{c_\infty} \right]^{-1} \\ \rightarrow \begin{cases} c_0, & \text{for } \omega\tau \ll 1, \\ c_\infty, & \text{for } \omega\tau \gg 1, \end{cases} \quad (19)$$

and

$$\bar{\alpha}_p = \frac{\omega}{\sqrt{2}} \left(\frac{1}{c_0} - \frac{1}{c_\infty} \right) \left\{ \frac{\sqrt{1 + \omega^2\tau^2} - 1}{1 + \omega^2\tau^2} \right\}^{1/2} \\ \rightarrow \begin{cases} \frac{\omega^2\tau}{2} \left(\frac{1}{c_0} - \frac{1}{c_\infty} \right) & \text{for } \omega\tau \ll 1, \\ \sqrt{\frac{\omega}{2\tau}} \left(\frac{1}{c_0} - \frac{1}{c_\infty} \right), & \text{for } \omega\tau \gg 1. \end{cases} \quad (20)$$

The value of the attenuation, $\bar{\alpha}_{pT}$, at the transition frequency, that is, when $\omega = 2\pi f_T = 1/\tau$, will be useful later as a normalizing factor. From Eq. (20),

$$\bar{\alpha}_{pT} = \frac{\sqrt{\sqrt{2}-1}}{2\tau} \left(\frac{1}{c_0} - \frac{1}{c_\infty} \right), \quad (21)$$

where, it should be noted, the term on the right is inversely proportional to τ .

Obviously, if c_∞ were infinite, Eq. (18) would reduce to the expression in Eq. (15) for a true viscous fluid. When c_∞ is finite, however, the MVF dispersion curves are almost identical in shape to those from the EDF model. In particular, the high-frequency phase speed from Eq. (19) asymptotes to c_∞ , in accord with the EDF model.

For a quantitative comparison of the two models, it is necessary to express the three parameters (c_0, c_∞, f_T) in terms of the eight material variables of the EDF model. This has already been done for c_0 in Eq. (13). From the asymptotic expansions of the Bessel functions in Eq. (8), it can be shown that the function F in Eq. (7) scales as $\sqrt{\omega\tau_0}$ in the limit of high frequency, and hence it follows from Eqs. (1) and (3) that

$$c_\infty = c_0 \sqrt{\frac{\rho_2\rho}{\rho_1\rho_f}}. \quad (22)$$

Unlike c_0 , the high-frequency phase speed, c_∞ , depends on the tortuosity, α , through the presence of the ratio ρ_2/ρ_1 under the radical in Eq. (22). Expressions equivalent to those in Eqs. (13) and (22) have been given by Williams,¹ although not in the context of the MVF model in Eq. (18).

The one remaining parameter to be identified in Eq. (18) is the transition frequency, $f_T = (2\pi\tau)^{-1}$. This is readily derived by expanding the MVF model [Eq. (18)] in a Taylor series to first order in $\omega\tau$.

$$\frac{1}{\bar{c}} = \frac{1}{c_0} \left[1 + \frac{i\omega\tau}{2} \frac{(c_\infty - c_0)}{c_\infty} - \dots \right]. \quad (23)$$

On equating the first-order term here to that in the Taylor series for the complex wave speed [Eq. (12)] from the EDF model, it is found that

$$\tau = \frac{\tau_0}{\beta} \left(\frac{\rho_2}{\rho_f} - \frac{\rho_1}{\rho} \right) \left(\frac{c_\infty}{c_\infty - c_0} \right). \quad (24)$$

Thus, the transition frequency, $f_T = (2\pi\tau)^{-1}$, scales as $(1/\tau_0)$, which, as has been shown in Eq. (6), is proportional to the ratio η/κ . It is also evident that τ depends on the porosity, β , and the tortuosity, α . Note that the transition frequency, f_T , differs from Biot's^{2,3} characteristic frequency, f_c , through the presence of the terms in round brackets in Eq. (24).

IV. COMPARISON OF THE EDF AND MVF MODELS

To compare the EDF and MVF models, it is convenient to plot the dispersion curves as functions of the dimensionless frequency, $\omega\tau_0/2\pi$. Then the phase speed and attenuation (normalized to $\bar{\alpha}_{pT}$) from both models are invariant to changes in the permeability and the pore-fluid viscosity. As for the remaining six material variables, we shall adopt the values shown in Table I, which are the same as in Williams.¹ With these material properties, the values of the three parameters characterizing the MVF model are $c_0 = 1607.6$ m/s, from Eq. (13), $c_\infty = 1752.1$ m/s, from Eq. (22), and $f_T = 266.46$ Hz ($\tau = 0.5973$ ms), from Eq. (24). The normalizing attenuation, from Eq. (21), is $\bar{\alpha}_{pT} = 0.24$ dB/m.

Figure 1 shows the phase speed normalized to c_0 and the attenuation normalized to $\bar{\alpha}_{pT}$ as functions of the normalized frequency, $\omega\tau_0$. The curves in Figs. 1(a) and 1(b) have been evaluated from the EDF model [Eq. (1)] and the MVF model [Eq. (18)]. As noted above, the shapes of these curves are universally valid for all values of permeability and pore-fluid viscosity. To convert the normalized frequencies along the abscissa to Hz, it is necessary only to multiply by the factor $\tau_0^{-1} = 10^4$ Hz for the particular values of the material variables in Table I. When the normalizing factors on the ordinates are backed out, the EDF curves in Fig. 1 are seen to be identical to those in Figs. 2 and 3 in Williams.¹

The normalized transition frequency in Fig. 1 takes the value $f_T\tau_0 = 0.02665$, which falls toward the lower end of the low- to high-frequency transition region of the EDF sound speed and attenuation curves (unlike Biot's normaliz-

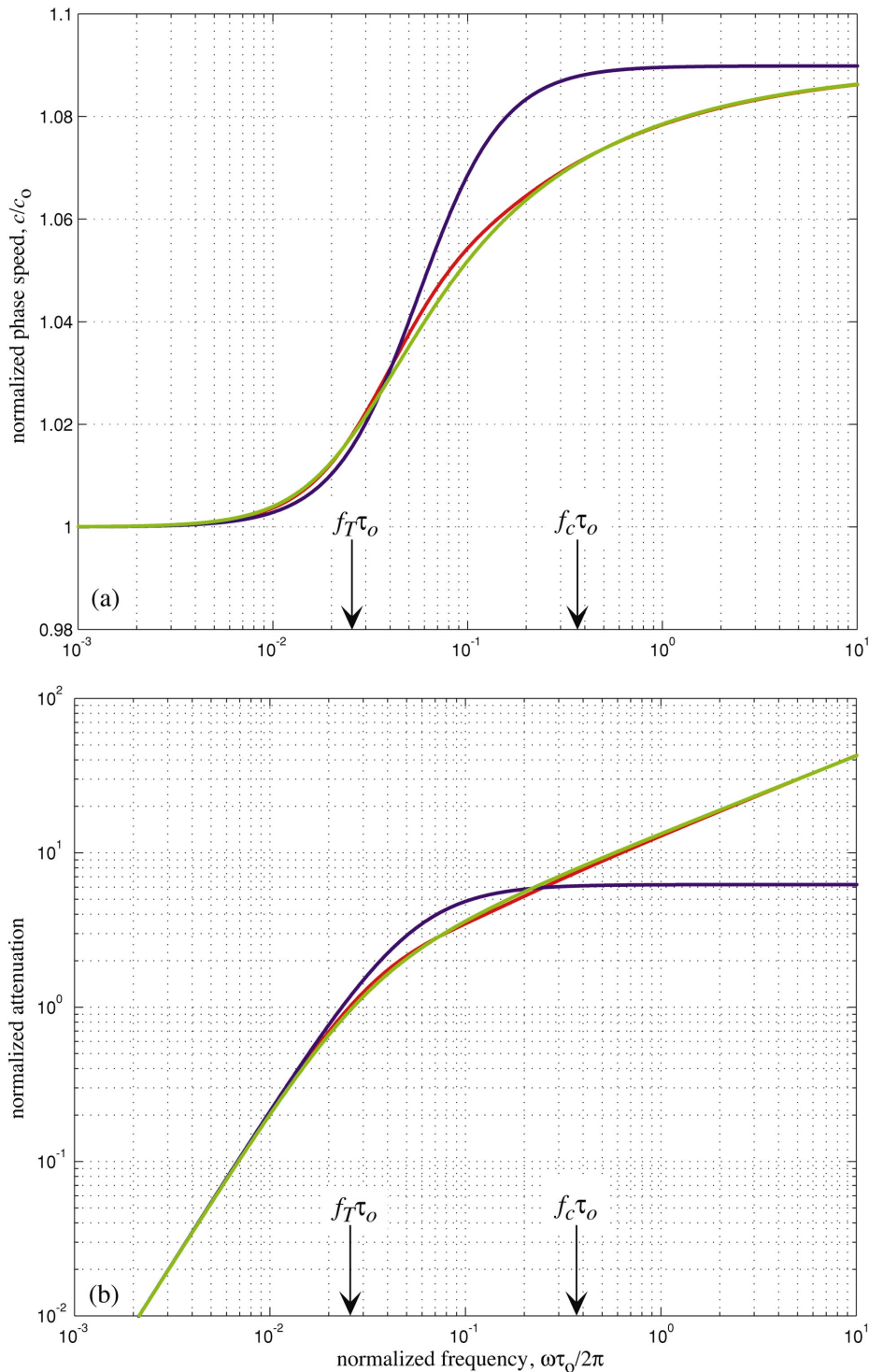


FIG. 1. Dispersion curves from the EDF model (red) and the MVF model (green) plotted as functions of normalized frequency $\omega\tau_0/2\pi$. (a) Phase speed normalized to c_0 and (b) attenuation normalized to $\bar{\alpha}_{pT}$. The blue curves are from the EDF model but with Biot's function F set to unity. The transition frequency, $f_T\tau_0$, and Biot's normalizing frequency, $f_c\tau_0=\beta$, are indicated on the frequency axes by the vertical arrows.

ing frequency, $f_c = \beta/\tau_0$, which falls well above the transition region). Thus, f_T provides a useful measure of the frequency at which the transition from low- to high-frequency behavior begins.

It is clear from Fig. 1 that the EDF and MVF models are indistinguishable at high and low frequencies, and are almost so at mid-frequencies, where the curves separate slightly but by little more than the thickness of the lines themselves. The

natural conclusion is that, at all frequencies, the algebraic, three-parameter MVF model provides a very good approximation to Biot's "fluid" theory, as expressed through the EDF model developed by Williams.¹

V. POROSITY AND TORTUOSITY

The normalizations in Fig. 1 are useful for making the comparison between the EDF and MVF models. For a me-

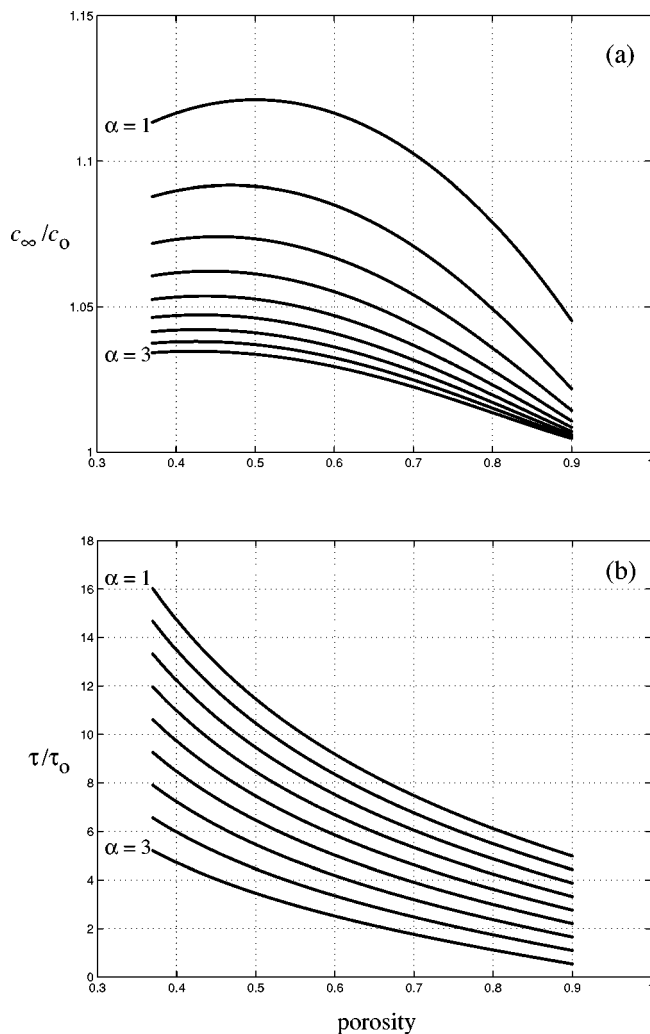


FIG. 2. The normalized variables a) c_∞/c_0 from Eq. (22) and b) τ/τ_0 from Eq. (24) as functions of porosity, with tortuosity, $\alpha=1,1.25,1.5,\dots,2.75,3$, treated as a parameter.

dium described by the material properties in Table I, the absolute values of phase speed and attenuation are readily obtained from Fig. 1 by multiplying the normalized ordinates by the respective normalizing factors, $c_0=1607.6$ m/s and $\bar{\alpha}_{pT}=0.24$ dB/m. In the following discussion, a simple scheme is outlined for evaluating the three parameters (c_0, c_∞, f_T) of the MVF model, and hence the normalizing factors, for a more general set of values for the material parameters.

Since the material constituents of many marine sediments are much the same, namely quartz–sand and seawater, the surficial densities, ρ_s and ρ_f , and bulk moduli, K_r and K_f , of the solid and fluid phases are more or less invariant (if minor temperature dependencies are neglected) from one sediment to another, with representative values as given in Table I. In contrast, the ratio of the permeability to the pore–fluid viscosity, κ/η , may vary by several orders of magnitude between sediments, primarily due to differences in the permeability¹⁵ and perhaps a weak temperature dependence exhibited by the viscosity of seawater. However, the effects of such variations on the wave properties predicted by the EDF model have already been taken into account by plotting

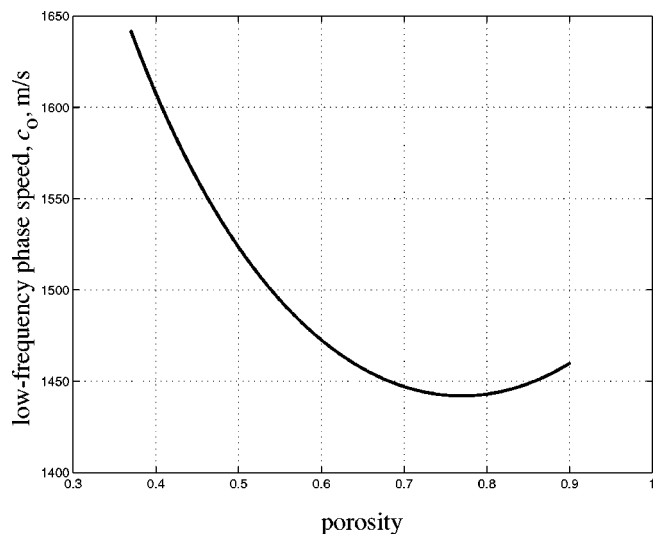


FIG. 3. Low-frequency (Wood's) phase speed, c_0 , as a function of porosity, from Eqs. (13), (2), and (4).

the dispersion curves (phase speed and normalized attenuation) in Fig. 1 as functions of the normalized frequency $\omega\tau_0$. Absolute frequency may be recovered once τ_0 has been determined from Eq. (6). This leaves only two variables still to be dealt with in Table I, the porosity, β , and tortuosity, α , of the granular medium, both of which may vary significantly from one sediment to another.

According to Stoll,¹⁵ the tortuosity (also known as the structure factor) may theoretically take values between 1 and 3; and, as summarized in Figs. 5, 6, and 9 of Buckingham,²¹ observations by Hamilton^{22,23} and Richardson^{24–26} indicate that the fractional porosity may lie anywhere between 0.37 and 0.85, with the larger-grained sediments tending toward lower porosities. The lower limiting value of the porosity is exhibited by the coarser sands and, at 0.37, is consistent with a random packing of smooth, uniform spheres.^{27,28} In the finer sediments, the rms roughness of the grains may be comparable with the grain diameter, thus permitting enhanced percolation of seawater between grains, which, according to a geometrical, random-packing model by Buckingham,²¹ could account for the higher values of porosity observed in the fine-grained materials.

Be that as it may, the normalized parameters (c_∞/c_0) and (τ/τ_0) vary with the porosity and the tortuosity (but not with the permeability or pore–fluid viscosity). The functional dependence of these parameters on porosity is plotted in Fig. 2, where each curve is associated with a fixed value of the tortuosity. The families of curves in Figs. 2(a) and 2(b) were computed from Eqs. (22) and (24), respectively. The low-frequency phase speed, c_0 , given by Wood's equation²⁰ [Eq. (13)], is independent of the tortuosity but varies with the porosity, as shown in Fig. 3.

Once the porosity and tortuosity of a sediment have been specified, the corresponding values of (c_∞/c_0), (τ/τ_0) and c_0 may be read from the curves in Figs. 2 and 3. Dispersion pairs (phase speed and absolute attenuation versus frequency) may then be computed directly from the MVF model in Eq. (18) for any set of values (representing sandy sediments) for the eight material variables. Alternatively,

since Figs. 2 and 3 yield the necessary normalizing factors, the absolute values of phase speed and attenuation at a spot frequency may be determined directly from the green curves in Fig. 1.

In the case of muds, silts and clays, where the density and bulk modulus of the mineral grains may vary significantly from one material to another, it is probably easier to abandon the graphical approach in favor of direct evaluation of the three parameters (c_0, c_∞, f_T) from Eqs. (13), (22), and (24). The phase speed and attenuation may then be computed directly from Eq. (18) or Eqs. (19) and (20).

VI. BIOT'S FLOW FUNCTION, F

It could be argued that the function F , introduced by Biot to account for the high-frequency departure from Poiseuille flow through the pores, is the most complicated part of the EDF model. As specified by Eqs. (7)–(10), F exhibits a frequency dependence that is not immediately apparent, since it involves the ratio of two Bessel functions of complex argument. Hence the effects of F on the dispersion curves are obscure, although it is fairly evident that the flow function has little influence at low frequencies, where it takes a value very close to unity.

To illustrate how F modifies the dispersion curves, the EDF model [Eq. (1)] has been evaluated with F set to unity at all frequencies. The result for the normalized phase speed and attenuation is illustrated by the blue curves in Fig. 1. Below the transition frequency (i.e., $f_T\tau_0 = 0.02665$ on the abscissa in Fig. 1), it is clear that F has a negligible effect on the phase speed and attenuation. At mid-frequencies, with $F = 1$, the phase speed is overestimated, as is the attenuation, but in both cases by no more than about 2%; and at high frequencies, the phase speed asymptotes to c_∞ , just as it does when using the full expression for F , but the attenuation becomes constant, independent of frequency, rather than diverging as $\omega^{1/2}$, as predicted by the complete EDF model.

Clearly, the effects of F on the dispersion curves are rather minor. Principally, the frequency dependence of F [Eqs. (7)–(10)] serves to ensure that the form of the attenuation predicted by the EDF model is, ironically, no different from that of a simple viscous fluid.

VII. CONCLUDING REMARKS

It is clear from the comparison of the EDF and MVF models that the dispersion curves predicted by the “fluid” Biot theory are constrained to take simple shapes that are governed by just three parameters, (c_0, c_∞, f_T). Two of these parameters, c_0 and c_∞ , are the phase speeds in the limit of low and high frequency, respectively, and the third, f_T , is a transition frequency that separates the high- and low-frequency regimes in the phase speed and attenuation curves. Embedded in these three parameters are the eight variables, listed in Table I, that describe the material properties of the saturated porous medium. Explicit, algebraic expressions have been derived for all three parameters [Eqs. (13), (22), and (24)], allowing the MVF model to be evaluated for any set of the material properties.

The transition frequency, f_T , scales inversely with a normalizing time, τ_0 , which itself is proportional to the ratio of the permeability to the pore–fluid viscosity (κ/ν). These two material properties appear nowhere in the “fluid” Biot theory outside τ_0 . In particular, the limiting low- and high-frequency phase speeds, c_0 and c_∞ , respectively, are independent of permeability and pore–fluid viscosity.

Taking as an example a typical sandy sediment represented by the values of the material properties in Table I, the normalizing time, τ_0 , from Eq. (6), is 0.1 ms and, from Eq. (24), the transition frequency is $f_T = (2\pi\tau)^{-1} = 266.5$ Hz. Much below this frequency, the EDF model predicts a sound speed close to c_0 and an attenuation scaling as f^2 ; and much above the sound speed asymptotes to c_∞ and the attenuation scales as $f^{1/2}$. It is, however, still an open question as to whether the measured dispersion curves of sandy marine sediments show a pronounced transition from low- to high-frequency behavior somewhere around several hundred Hertz. This is an issue that has recently been the subject of debate within ONR's SAX99 research initiative on the interaction of sound with marine sediments.^{14,29}

An alternative possibility, and one that is consistent with a grain-shearing argument,¹¹ is that no such transition occurs, and instead the phase speed and attenuation curves show more or less constant (log–log) gradients at all frequencies, including the band between 0.1 and 1 kHz. It is not easy, however, to measure the dispersion at frequencies below 1 kHz with sufficient precision to distinguish between the two theoretical predictions. New techniques that are currently under development,^{30,31} involving a high-Doppler, airborne sound source (a propeller-driven aircraft) and acoustic sensors buried in the sediment, may yield sufficiently precise estimates of the phase speed and attenuation in the frequency band 0.1–1 kHz to resolve the issue.

ACKNOWLEDGMENTS

This work was supported by Dr. J. Simmen and Dr. E. Livingston, Ocean Acoustics Code, the Office of Naval Research, under Grants No. N00014-93-1-0054 and No. N00014-04-1-0063.

¹K. L. Williams, “An effective density fluid model for acoustic propagation in sediments derived from Biot theory,” *J. Acoust. Soc. Am.* **110**, 2276–2281 (2001).

²M. A. Biot, “Theory of propagation of elastic waves in a fluid-saturated porous solid: I. Low-frequency range,” *J. Acoust. Soc. Am.* **28**, 168–178 (1956).

³M. A. Biot, “Theory of propagation of elastic waves in a fluid-saturated porous solid: II. Higher frequency range,” *J. Acoust. Soc. Am.* **28**, 179–191 (1956).

⁴M. D. Richardson *et al.*, “Overview of SAX99: environmental considerations,” *IEEE J. Ocean. Eng.* **26**, 26–53 (2001).

⁵H. J. Simpson and B. H. Houston, “A synthetic array measurement of a fast compressional and a slower wave in an unconsolidated water-saturated porous medium,” *J. Acoust. Soc. Am.* **102**, 3210 (1997).

⁶H. J. Simpson and B. H. Houston, “Analysis of laboratory measurements of sound propagating into an unconsolidated water-saturated porous media,” *J. Acoust. Soc. Am.* **103**, 3095–3096 (1998).

⁷H. J. Simpson, B. H. Houston, and L. S. Couchman, “Measurements and modeling of sound propagating into unconsolidated water-saturated porous media in a laboratory environment,” *J. Acoust. Soc. Am.* **104**, 1787 (1998).

⁸H. J. Simpson and B. H. Houston, “Synthetic array measurements of

- acoustical waves propagating into a water-saturated sandy bottom for a smoothed and a roughened interface," *J. Acoust. Soc. Am.* **107**, 2329–2337 (2000).
- ⁹T. J. Plona, "Observation of a second bulk compressional wave in a porous medium at ultrasonic frequencies," *Appl. Phys. Lett.* **36**, 259–261 (1980).
- ¹⁰D. L. Johnson and T. J. Plona, "Acoustic slow waves and the consolidation transition," *J. Acoust. Soc. Am.* **72**, 556–565 (1982).
- ¹¹M. J. Buckingham, "Wave propagation, stress relaxation, and grain-to-grain shearing in saturated, unconsolidated marine sediments," *J. Acoust. Soc. Am.* **108**, 2796–2815 (2000).
- ¹²M. J. Buckingham, "Acoustic pulse propagation in dispersive media," in *New Perspectives on Problems in Classical and Quantum Physics. Part II. Acoustic Propagation and Scattering—Electromagnetic Scattering*, edited by P. P. Delsanto and A. W. Sáenz (Gordon and Breach, Amsterdam, 1998), Vol. 2, pp. 19–34.
- ¹³J. E. White, *Underground Sound: Application of Seismic Waves* (Elsevier, Amsterdam, 1983).
- ¹⁴M. J. Buckingham and M. D. Richardson, "On tone-burst measurements of sound speed and attenuation in sandy marine sediments," *IEEE J. Ocean. Eng.* **27**, 429–453 (2002).
- ¹⁵R. D. Stoll, *Sediment Acoustics* (Springer-Verlag, Berlin, 1989).
- ¹⁶M. D. Collins, W. A. Kuperman, and W. L. Siegmund, "A parabolic equation for poro-elastic media," *J. Acoust. Soc. Am.* **98**, 1645–1656 (1995).
- ¹⁷J. L. Williams, "Ultrasonic wave propagation in cancellous and cortical bone: Prediction of some experimental results by Biot's theory," *J. Acoust. Soc. Am.* **91**, 1106–1112 (1992).
- ¹⁸Y. Mu, M. Badiey, and A. H.-D. Cheng, "Parameter uncertainty analysis on acoustic response in fluid filled poroelastic media," *J. Acoust. Soc. Am.* **106**, 151–163 (1999).
- ¹⁹D. L. Johnson, J. Koplik, and R. Dashen, "Theory of dynamic permeability and tortuosity in fluid-saturated porous media," *J. Fluid Mech.* **176**, 379–402 (1987).
- ²⁰A. B. Wood, *A Textbook of Sound*, 3rd ed., p. 361, Eq. (3) (Bell and Sons, London, 1964).
- ²¹M. J. Buckingham, "Theory of acoustic attenuation, dispersion, and pulse propagation in unconsolidated granular materials including marine sediments," *J. Acoust. Soc. Am.* **102**, 2579–2596 (1997).
- ²²E. L. Hamilton, "Sound velocity and related properties of marine sediments, North Pacific," *J. Geophys. Res.* **75**, 4423–4446 (1970).
- ²³E. L. Hamilton, "Compressional-wave attenuation in marine sediments," *Geophysics* **37**, 620–646 (1972).
- ²⁴M. D. Richardson, "Spatial variability of surficial shallow water sediment geoacoustic properties," in *Ocean-Seismo Acoustics: Low-Frequency Underwater Acoustics*, edited by T. Akal and J. M. Berkson (Plenum, New York, 1986), pp. 527–536.
- ²⁵M. D. Richardson and K. B. Briggs, "On the use of acoustic impedance values to determine sediment properties," in *Acoustic Classification and Mapping of the Seabed*, edited by N. G. Pace and D. N. Langhorne (University of Bath, Bath, 1993), Vol. 15, pp. 15–24.
- ²⁶M. D. Richardson and K. B. Briggs, "In situ and laboratory geoacoustic measurements in soft mud and hard-packed sand sediments: Implications for high-frequency acoustic propagation and scattering," *Geo-Mar. Lett.* **16**, 196–203 (1996).
- ²⁷O. K. Rice, "On the statistical mechanics of liquids, and the gas of hard elastic spheres," *J. Chem. Phys.* **12**, 1–18 (1944).
- ²⁸M. R. Wyllie, A. R. Gregory, and L. W. Gardner, "Elastic wave velocities in heterogeneous and porous media," *Geophysics* **21**, 41–70 (1956).
- ²⁹K. L. Williams, D. R. Jackson, E. I. Thorsos, D. Tang, and S. G. Schock, "Comparison of sound speed and attenuation measured in a sandy sediment to predictions based on the Biot theory of porous media," *IEEE J. Ocean. Eng.* **27**, 413–428 (2002).
- ³⁰M. J. Buckingham, E. M. Giddens, J. B. Pompa, F. Simonet, and T. R. Hahn, "Sound from a light aircraft for underwater acoustics experiments?," *Acta Acustica united with Acustica* **88**, 752–755 (2002).
- ³¹M. J. Buckingham, E. M. Giddens, F. Simonet, and T. R. Hahn, "Propeller noise from a light aircraft for low-frequency measurements of the speed of sound in a marine sediment," *J. Comput. Acoust.* **10**, 445–464 (2002).